Portrait Sculptures of Augustus: Categorization via Local Shape Comparison

Min Lu*, Yujin Zhang*, Bo Zheng*, Takeshi Masuda†, Shintaro Ono*,
Takeshi Oishi*, Kyoko Sengoku-Haga‡ and Katsushi Ikeuchi*
*Institute of Industrial Science, The University of Tokyo, Japan
Email: {lumin, yjzhang, zheng, onoshin, oishi, ki}@cvl.iis.u-tokyo.ac.jp
† National Institute of Advanced Industrial Science and Technology, Japan
Email: t.masuda@aist.go.jp
‡ Graduate School of Arts and Letters, Tohoku University, Japan
Email: khaga@sal.tohoku.ac.jp

Abstract—**3D shape comparison with digital copies draws increasing attention in modern culture heritage studies. In this paper, we focus on analyzing portrait sculptures of Augustus with 3D scanned data. A feasible framework of automatic object categorization is proposed based on shape comparison, where distinguishing regions are simultaneously detected as well. High coincidence between our result and previous archaeological speculations is observed in validation experiments, which confirms the validity of the proposed method.**

I. INTRODUCTION

Augustus, the founder and first emperor of the *Roman Empire*, was worshiped by a large number of his statues scattered throughout the empire. These sculptures have been arousing people's attention for centuries.

The portrait sculptures of Augustus can be divided into several subcategories based on a certain criteria. For instance, in the pioneering work [1], busts of Augustus were roughly classified according to the style of forehead hair. At least three principal types were found, named as *Alcudia*, *Forbes* and *Prima Porta* respectively, as shown in Fig. 1. Generally speaking, the most canonical type, *Prima Porta*, is accompanied with close hair pincer. In contrast, forehead hair of *Alcudia* type portraits looks more fluffy, and *Forbes* type samples have a more widely apart hair pincer with a trace of uneasy expression as well. Notice that although this classification is widely accepted by most archaeologists, it has not been a final verdict yet. Different classification criteria lead to different results. For instance, another two different categorization proposals are presented in studies [2] and [3] respectively.

A. Motivation

We are inspired to explore the study of sculpture categorization, aiming to develop a fully data-driven categorization method, which is reliable for portrait sculptures. In particular, we want to extract feature regions that distinguish subcategories from each other. These regions are also called *distinguishing regions* or *feature regions* in the following sections.

B. Related Work

Digital archiving technique plays an increasingly important role in recent archaeological studies. Several studies of ana-
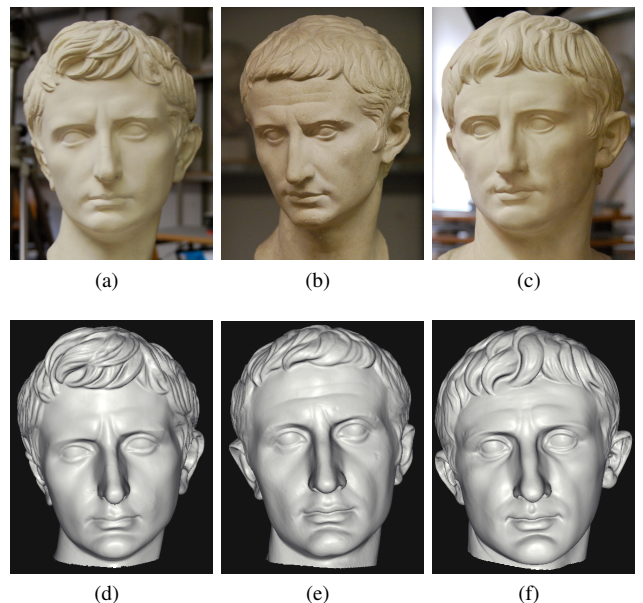

Fig. 1. Three representative portrait sculptures of Augustus from the *Museum of Casts of Classical Sculptures* in Munich. They belong to three principal type—*Alcudia*, *Forbes* and *Prima Porta* respectively. (a), (b) and (c) are photographs, while (d), (e) and (f) are images rendered from digital copies.

lyzing the sculptural reproduction via 3D shape comparison have been proposed. For example, taking use of craniofacial landmarks registration, the hypothesis that *Getty Augustus* was re-carved from an earlier portrait of *Caligula* is proven to be incorrect [4]. In another study [5], a numerical measurement of similar statues are developed, with an application to estimate the attribution of a classical sculpture named *Amazon Sciarra*.

Shape matching provides an effective way to compare similar objects, where accurate correspondences can be acquired. As an active research topic, several different approaches have been proposed. For example, in the shape normalization method, such as [6], objects are first embedded into canonical form and then compared directly. Although this method is sensitive to topological noise, it is extremely suitable for comparing isometric deformed objects. In case that target objects vary a lot but semantically similar, skeleton-based method can

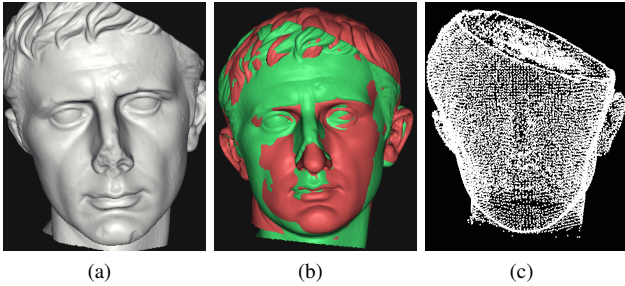(a)   (b)   (c)

Fig. 2. An illustration of the shape matching process. In this example, the head part of the *Augustus of Prima Porta*, shown in Fig. 1(f), was used as template sample. (a): the target shape; (b): non-rigid registration between target and template samples; (c): the corresponding points on (a), obtained via a *nearest neighbour* searching.

be employed to extract satisfactory correspondences. One of the representative studies is [7]. For more detailed discussion on this topic, a comprehensive survey is given in [8].

Besides, mesh segmentation is important to shape analysis as well. Clustering-based approach are proposed in [9] and [10]. A more recent study focus on co-segmentation of 3D shapes is introduced in [11], where subspace clustering is utilized. Different from our problem, these studies focus on dividing one or more objects into meaningful patches, while we pay more attention to locate where are the regions that distinguish one subcategory from the others.

C. Contribution

In this paper, we focus on the categorization problem within a group of similar objects. We digitized selected portrait sculptures of Augustus from the *Museum of Casts of Classical Sculptures* in Munich. With the obtained digital copies, a feasible shape comparison scheme is proposed. Different from traditional method where only overall similarity is available, we enrich the comparison with local shape similarity at each corresponding position. Meanwhile, feature regions that distinguish subcategories from each other can also be detected.

II. FRAMEWORK

A. Data acquisition and preprocessing

Given a set of sculptures for comparison, we need to obtain their accurate shape information first. In our case, we utilize 3D modeling techniques introduced in [12] and [13].

Before starting the comparison, the original data has to be processed to fit some requirements. For sculptures, this includes shape alignment and matching. Similar to the pre-processing step described in [14], all samples are first rigidly aligned together with auto-scaling, and then matched to a certain template with non-rigid transformation in order to obtain dense correspondences between them. Fig. 2 gives an illustration of this matching process. Compared with other shape matching methods, this approach is both simple and fast.

B. Distinguishing region detection via clustering

Traditionally, when comparing a group of objects, a *distance/similarity matrix* similar to the one in Fig. 3 is utilized
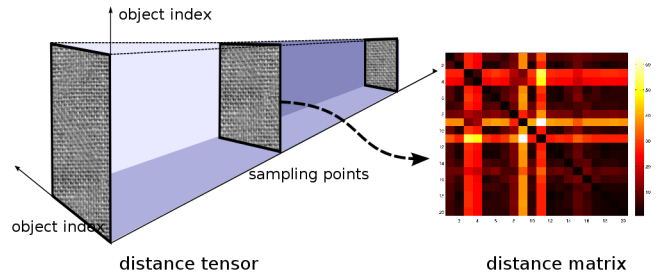

Fig. 3. The construction of distance tensor. Along the direction of sampling points, each slide itself is a distance matrix at a certain sampling point.

to evaluate pairwise overall distance/similarity. However, since we have already obtained dense correspondences between objects, actually similarities can be evaluated at every sampling points. Thus with an extra dimension of sampling positions, we extend the traditional distance matrix representation to the tensor form, which is called *distance tensor* in this paper.

Fig. 3 illustrates the construction process of distance tensor. Suppose the given data set contains M similar objects $\{O\}_{i=1}^{M}$ with N corresponding positions $\{P\}_{i=1}^{N}$. First, for each P_i we calculate a distance matrix D_i to record displacements between all pairs of objects at that position. Then we combine these distance matrices $\{D\}_{i=1}^{N}$ together to form a tensor, denoted as $\mathcal{T}_{M \times M \times N}$. Each sampling point is assigned with a distance matrix, which is a $M \times M$ square matrix D_i.

With this distance tensor $\mathcal{T}$, richer information compared with the traditional approach can be estimated during shape comparison. For instance, we can not only divide the data set into subcategories, but also locate which region makes one subcategory different from others. In order to detect these distinguishing regions, proper segmentation of the shape based on similarities among corresponding regions is required.

Similar to the study in [9], we utilize cluster analysis to detect distinguishing regions. However, the similarity evaluation between points in our method is different from those mesh segmentation method. Consider two arbitrary positions in the corresponding points set, denoted as P and Q. The distance between them is defined as:

$$dist(P, Q) = dist_{\mathbf{IMED}}(D_P, D_Q), \tag{1}$$

where D_P and D_Q are distance matrices at positions P and Q respectively. $dist_{\mathbf{IMED}}(\cdot)$ is a variation of Euclidean distance introduced in [15], where spatial relationships of matrix entries are taken into account as well.

An intuitive example can be used to explain why distinguishing region between different subcategories can be detected via clustering. Consider a problem of clustering facial profiles, as shown in Fig. 4. This data set is extremely simple, with four human profiles from two subcategories—one with smaller noses while the other with larger noses. $\{A_i\}_{i=1}^{4}$, $\{B_i\}_{i=1}^{4}$ and $\{C_i\}_{i=1}^{4}$ are three groups of corresponding points at different sampling positions. For simplicity, identical profiles are used within each subcategory. Actually the only difference between all these four samples is the shape of nose, which is shown in the aligned result. Therefore the nose part is the
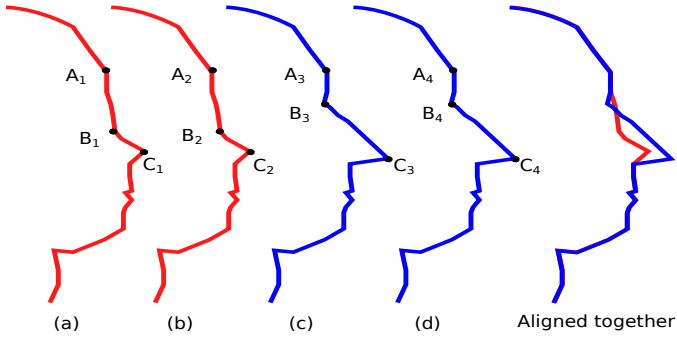
Fig. 4. An example of distinguishing feature in profile categorization. Four human profiles are used, where (a) and (b) are exactly the same, and the same as (c) and (d). $\{A_i\}_{i=1}^4$, $\{B_i\}_{i=1}^4$ and $\{C_i\}_{i=1}^4$ are three groups of corresponding points. In this example, the only distinguishing region is the nose, where $\{B_i\}_{i=1}^4$ and $\{C_i\}_{i=1}^4$ are included.

distinguishing region we want to detected.

Then we calculate distance matrices at all these three sampling positions separately. Take the first group $\{A_i\}_{i=1}^4$ as an example. The displacement between a certain pair of points, e.g. A_1 and A_2, is evaluated based on the aligned profiles. Since the positions of these two points coincide, the displacement $dist_{A_1,A_2}$ equals to zero.

The obtained distance matrices are visualized as heat maps in Fig. 5. It clearly shows that in the sense of comparing distance matrices within each group, $\{B_i\}_{i=1}^4$ and $\{C_i\}_{i=1}^4$ are more "similar" to each other compared with $\{A_i\}_{i=1}^4$. This result is consistent with the fact that only $\{B_i\}_{i=1}^4$ and $\{C_i\}_{i=1}^4$ locate in the distinguishing region—the nose. This demonstrates how it works to extract feature regions via cluster analysis.

In practice, considering that the number of sampling points is usually a relatively large number for cluster analysis, we utilized the spectral clustering method [16] to speed up the calculation.

III. Experiments

In our experiment, 12 well kept portrait sculptures of Augustus from the *Museum of Casts of Classical Sculptures* in Munich were used, as demonstrated in Fig. 8. Their digital copies were acquired by *Konica Minolta "Vivid 9i"* 3D laser scanner, with a very high measurement accuracy of $\pm 50 \mu m$. Since this categorization depends mainly on the front side, here we compared only the facial part as well as part of the hair near the forehead. About 50,000 uniformly sampled points on template sample were used for shape matching.

Fig. 6(b) gives one result of the detected feature regions. Notice that the number of clusters is manually assigned. In this example, this number was set to 12 and therefore the facial part was divided into 12 patches. Besides, in repeated experiments, even if the number of clusters is fixed, output results might not always be the same. This is due to the random initialization of spectral clustering. However, a dominant result will still be stable among all these outputs.

Taking into account that the forehead hair part is considered to be important in previous archaeological studies, here we
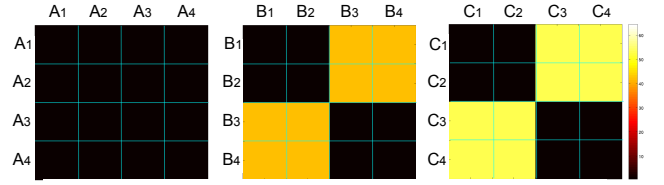

Fig. 5. A visualization of distance matrices in the example shown in Fig. 4. From left to right, these three heat maps correspond to sampling points $\{A_i\}_{i=1}^4$, $\{B_i\}_{i=1}^4$ and $\{C_i\}_{i=1}^4$ respectively. The lighter color is, the larger displacement it represents. Black corresponds to zero. It is clear that the latter two matrices are more similar to each other compared with the first one.

show the categorization result within this region as an example. Fig. 7 shows the average distance matrix within that patch as well as the hierarchical clustering result. The clustering result is further visualized in Fig. 8, where samples are dyed according to the categorization result shown in Fig. 7(b).

From this result, first we observed that the top left sculpture shown in Fig. 8, which is called *Capito413* for convenience, has the longest distance from other samples within this feature region. Notice that it is also the only *Alcudia* type sample in this data set. According to previous archaeological studies, portraits belonged to this type is supposed to have different forehead hair style from other types. Second, all portraits dyed with the blue color belong to the *Prima Porta* type. In particular, actually the heads of *PP* and *Chiusi* are very close to each other almost in every patches, which was also noted in [2]. These facts confirm the validity of the method we proposed.

IV. Summary

In this paper, a feasible solution for sculpture categorization is proposed. With the obtained corresponding points on digital copies, distinguishing feature regions are detected while categorization. We verified our method with a data set of the portrait sculptures of Augustus and we believe it can be applied to other shape comparison cases as well.

There are several limitations of the proposed method. First, the number of clusters is manually assigned in the step of feature region detection. Second, as a fast approximation to acquire corresponding points, our shape matching method might

Fig. 6. The result of distinguishing region detection. (a): an input model; (b): detected feature regions. Number of clusters is set to 12 in this example.
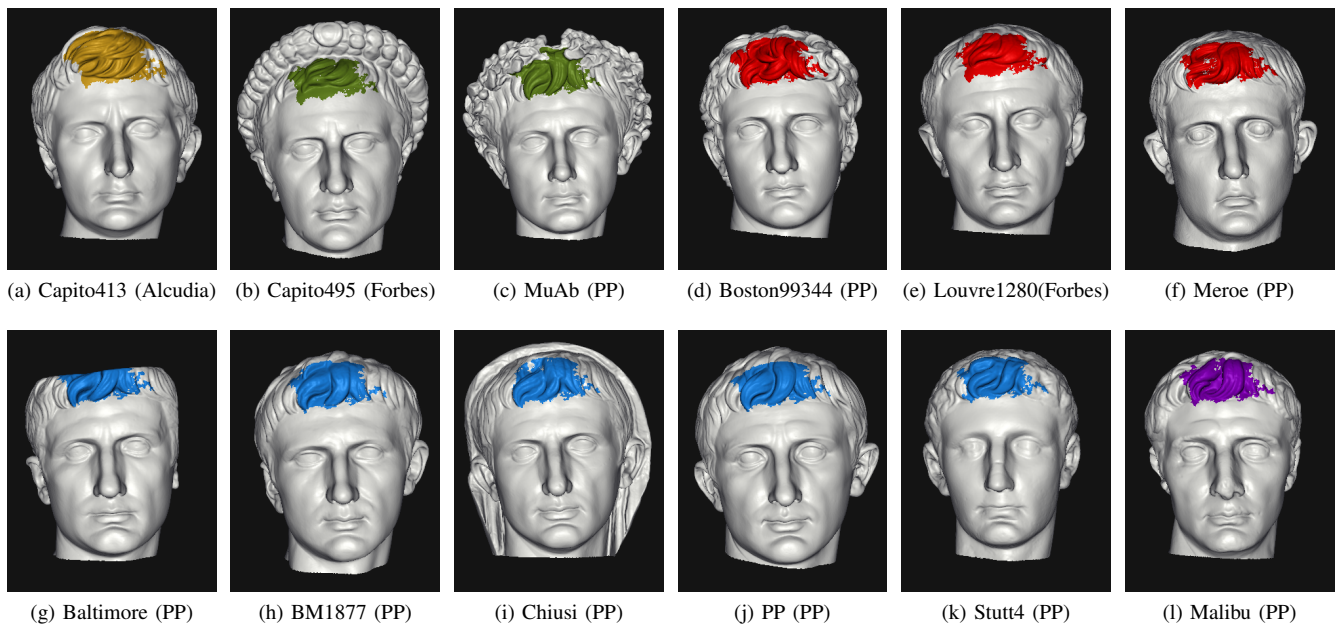
Fig. 8. Visualization of the categorization result in the forehead hair patch. Reference category labels given by archaeologists are also indicated in parentheses. Here "PP" is the abbreviation of "Prima Porta".
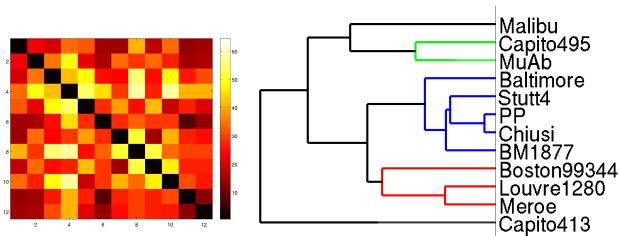

Fig. 7. A demonstration of average distance matrix and hierarchical clustering result within a certain cluster. This example corresponds to the forehead hair patch shown in Fig. 6(b), which is colored in cyan.

not be as accurate as the current state-of-the-art algorithm. We will try to improve these parts in future work.

REFERENCES

[1] M. Pfanner, "Über das Herstellen von Porträts," *Jahrbuch des Deutschen Archäologischen Instituts*, vol. 104, pp. 157–257, 1989.

[2] D. Boschung, *Die Bildnisse des Augustus*. Gebr. Mann Verlag, Berlin, 1993.

[3] J. Pollini, "The augustus from prima porta and the transformation of the polykleitan heroic ideal: The rhetoric of art," in *Polykleitos, the Doryphoros, and Tradition*, W. G. Moon, Ed. The University of Wisconsin Press, 1995.

[4] W. Storage. Augustus once and for all. [Online]. Available: http://www.rome101.com/Portraiture/Augustus/IsItRecarved/

[5] Y. Zhang, M. Lu, B. Zheng, T. Masuda, S. Ono, T. Oishi, K. Sengoku-Haga, and K. Ikeuchi, "Classical sculpture analysis via shape comparison," in *Proceedings of the 2013 International Conference on Culture and Computing*, 2013.

[6] A. Elad and R. Kimmel, "On bending invariant signatures for surfaces," *IEEE Trans. Pattern Anal. Mach. Intell.*, vol. 25, no. 10, pp. 1285–1295, Oct. 2003.

[7] O. K.-C. Au, C.-L. Tai, D. Cohen-Or, Y. Zheng, and H. Fu, "Electors voting for fast automatic shape correspondence," *Comput. Graph. Forum*, vol. 29, no. 2, pp. 645–654, 2010.

[8] O. van Kaick, H. Zhang, G. Hamarneh, and D. Cohen-Or, "A survey on shape correspondence," *Computer Graphics Forum*, vol. 30, no. 6, pp. 1681–1707, 2011.

[9] R. Liu and H. Zhang, "Segmentation of 3D meshes through spectral clustering," in *Proceedings of the Computer Graphics and Applications, 12th Pacific Conference*, ser. PG '04. Washington, DC, USA: IEEE Computer Society, 2004, pp. 298–305.

[10] S. Katz and A. Tal, "Hierarchical mesh decomposition using fuzzy clustering and cuts," *ACM Trans. Graph.*, vol. 22, no. 3, pp. 954–961, Jul. 2003.

[11] R. Hu, L. Fan, and L. Liu, "Co-segmentation of 3D shapes via subspace clustering," *Computer Graphics Forum (Proceedings of SGP)*, vol. 31, no. 5, pp. 1703–1713, 2012.

[12] K. Ikeuchi, T. Oishi, J. Takamatsu, R. Sagawa, A. Nakazawa, R. Kurazume, K. Nishino, M. Kamakura, and Y. Okamoto, "The Great Buddha project: Digitally archiving, restoring, and analyzing cultural heritage objects," *Int. J. Comput. Vision*, vol. 75, no. 1, pp. 189–208, 2007.

[13] T. Masuda, "Registration and integration of multiple range images by matching signed distance fields for object shape modeling," *Comput. Vis. Image Underst.*, vol. 87, no. 1-3, pp. 51–65, Jul. 2002.

[14] M. Lu, B. Zheng, J. Takamatsu, K. Nishino, and K. Ikeuchi, "Preserving the Khmer smile: Classifying and restoring the faces of Bayon," in *Proceedings of the 12th International conference on Virtual Reality, Archaeology and Cultural Heritage*, ser. VAST'11, 2011, pp. 161–168.

[15] L. Wang, Y. Zhang, and J. Feng, "On the euclidean distance of images," *IEEE Trans. Pattern Anal. Mach. Intell.*, vol. 27, no. 8, pp. 1334–1339, 2005.

[16] U. Luxburg, "A tutorial on spectral clustering," *Statistics and Computing*, vol. 17, no. 4, pp. 395–416, Dec. 2007.